Applied Catalysis B: Environmental 160–161 (2014) 480–491

Contents lists available at ScienceDirect

Applied Catalysis B: Environmental

journal homepage: www.elsevier.com/locate/apcatb

DME, propane and CO: The oxidation, steam reforming and WGS over Pt/Al_2O_3. The effect of aging and presence of water

Oana Mihai[a,b], Anna Fathali[a,c], Xavier Auvray[a], Louise Olsson[a,*]

[a] Chemical Reaction Engineering and Competence Centre for Catalysis, Chalmers University of Technology, SE-412 96 Göteborg, Sweden
[b] Department of Petroleum Processing Engineering and Environmental Protection, Petroleum-Gas University of Ploiesti, 39 Bucuresti Bd., 100680 Ploiesti, Romania
[c] Volvo Car Corporation, SE-405 31 Göteborg, Sweden

ARTICLE INFO

Article history:
Received 18 December 2013
Received in revised form 14 May 2014
Accepted 26 May 2014
Available online 2 June 2014

Keywords:
Hydrocarbons
Pt/Al_2O_3
Aging
WGS
Steam reforming

ABSTRACT

The effect of aging in two environments (Ar at 800 °C and $SO_2 + NO + O_2 + H_2O$ at 250 °C) on oxidation/steam reforming reactions using dimethyl ether (DME), propane and CO were investigated on Pt/Al_2O_3 catalysts. Platinum dispersion as well as the changes in Pt-particles sizes were examined. The BET surface area of aged catalysts decreased compared to the fresh (degreened) sample, indicating that aging in inert gas may collapse some pores in alumina and for aging in sulfur atmosphere it may block some pores of the catalysts. Using SEM/EDX, higher sulfur amount was found in the inlet position of the aged sulfur monolith and it decreased linearly with the direction of the flow along the monolith length. The effect of water was also studied and it was found that propane and DME oxidation is negatively influenced by the presence of water, while for CO an increased activity was found. Thermal aging of the Pt/Al_2O_3 catalyst resulted in quite small deactivation for the examined reactions. The dispersion after the sulfur aging, and subsequent H_2 reduction, was the same as after the thermal aging at 800 °C, but interestingly the activity is significantly different. After the sulfur aging and hydrogen regeneration, the DME and C_3H_8 oxidation is promoted, while CO oxidations are slightly inhibited in the presence of water. The effect of the sulfur aging had a minor effect on DME-SR, while it completely deactivated steam reforming for propane. For the WGS reaction, the sulfur aging resulted in an overall decreased activity and in addition the conversion went through a maximum. We suggest that residues of sulfur on the alumina inhibit the water activation in the WGS reaction.

1. Introduction

Vehicles equipped with diesel engines have high efficiency and thereby low fuel consumption. The rigorous environmental regulations on diesel engine emissions requires further development of the exhaust after-treatment technology, which lowers the emission levels of the pollutants (nitrogen oxides NO_x, carbon monoxide, unburned hydrocarbons (HC) and particulate matter (PM)) [1,2]. Promising technologies for NO_x after-treatment are lean NO_x-traps (LNT; also called (NO_x) storage-reduction (NSR) catalytic system) [3] and selective catalytic reduction (SCR) [4,5]. Instead of using diesel fuel, another effective option is to use dimethyl ether (DME), as alternative clean fuel. DME has the advantage of that it can be produced from biomass, which is important in order to reduce the use of oil and thereby reducing the global warming. It is also possible to produce DME from other feed-stocks, such as natural gas, crude oil and coal [6,7]. DME has high H/C ratio, high energy density, low boiling point, and high oxygen content [2,8].

The DME steam reforming (DME SR) is highly endothermic process and high amount of hydrogen is produced [9–11], while the oxidation/partial oxidation of DME is exothermic. Two mechanistic pathways are considered for DME oxidation: the decomposition of DME followed by the oxidation of decomposed species and the direct oxidation of DME by oxygen [12–14]. DME partial oxidation and steam reforming were mainly studied over reforming catalysts (Ni/Al_2O_3) or noble metals (Rh, Pt) supported on Al_2O_3 and high conversion is obtained. The addition of other materials (Li^+, Na^+, K^+) lowered the DME activity and hydrogen yield [15]. Furthermore, Solymosi et al. [16] showed that the specific activity of noble metals in the catalytic complete DME oxidation increased in the following order Ru > Pt > Ir > Pd > Rh. The reaction takes place above 400 K and Ru and Pt were found to be the most effective catalysts [16].

* Corresponding author. Tel.: +46 31 772 4390; fax: +46 31 772 3035.
E-mail address: louise.olsson@chalmers.se (L. Olsson).

http://dx.doi.org/10.1016/j.apcatb.2014.05.048
0926-3373/

Furthermore, catalytic oxidation of saturated and unsaturated hydrocarbons (e.g. propane and propene) has become the focus of many studies due to its importance in emission control and for energy production. Propane is a typical industrial flue gas, which is present in liquefied petroleum gas (LPG) powered vehicles [17–19]. Various catalytic systems for propane oxidation have been studied, for example Au on MO_x/Al_2O_3 (where M:Cu and Co) [20]. Due to their large oxygen storage capacity, CeO_2–ZrO_2 mixed oxides [21], alumina supported CuO–CeO_2 [22,23] or other non-noble metal mixed oxides catalysts (Fe, Mn, Co) are also used as alternative oxidation catalysts [24,25]. Currently, platinum group catalysts are widely employed due to their high oxidation activity at low temperatures [26–30] compared to transition metal oxide-based catalysts. In order to enhance the catalytic activity of platinum on propane combustion, many studies have been focused either on the effect of different catalytic support materials (Al_2O_3, MgO, SiO_2–Al_2O_3) [31,32] or on the role of particle size and metal dispersion [27,33]. Yoshida et al. [32] concluded that the catalytic activity varies with both acid strength of the supports and the platinum dispersion, while Otto et al. [27] noticed that the oxidation of propane on Pt/γ-alumina is a structure sensitive reaction and the reaction rate increases with Pt particle size. Propene, due to its double bond, is more reactive than propane. The catalytic combustion of these two hydrocarbons, where propene shows lower light-off temperature than propane [34,35] demonstrates this fact. However, the presence of propene on the catalytic surface may be detrimental for other desired reactions such as NO oxidation [36] and CO oxidation [37].

Two relevant reactions with environmental and industrial interest are CO oxidation, to produce CO_2, and water gas-shift (WGS), where CO is reacting with water to produce hydrogen and CO_2. Noble metals (Pt, Au) and copper catalysts are active materials for CO oxidation [38–40], as well as for low-temperature WGS [41,42]. However, Pt-supported catalysts have been preferred due to their superior activity for low temperature CO oxidation [43] and their high turnover rates (TOF) for CO in WGS [44,45]. In addition, Pt-supported catalysts (on Al_2O_3, CeO_2) are the most widely used materials for abatement of volatile compounds (VOC).

A large number of studies have focused on the sintering phenomenon of Pt-based DOC catalyst depending on aging conditions [46–49]. The thermal aging was found to have a crucial impact on the size, morphology and distribution of platinum particles. Furthermore, the sintering of platinum crystallites at elevated temperatures coupled with the dispersion changes were observed [50,51]. Kim et al. [52] studied the thermal aging under nitrogen and oxygen atmospheres at 850 °C using different aging times and the sintering of the active metal as well as the support structure were observed. Matam et al. [53] investigated the evolution of Pt/Al_2O_3 during aging at 800 °C under different conditions (air and simulated lean diesel exhaust gas mixture consisting of CO, CO_2, O_2, NO, C_3H_6, C_3H_8, diluted in N_2) and lowest platinum dispersion upon aging in air was found. The morphology of platinum nanoparticles is changed and is strongly dependent on the aging treatment, showing that spherical platinum particles are formed under thermal aging in oxidizing atmosphere whereas the cuboctahedral nanoparticles were found during aging under lean exhaust environment [53].

The effect of long time exposure to SO_2 at low temperature (250 °C) over Pt-based monolith catalysts has been investigated by Olsson and Karlsson [54] and Auvray et al. [55], concluding that SO_2 aging causes a large sintering and migration of platinum particles. The deactivation of Pt/Al_2O_3 by sulfate formation was observed by Kolli et al. [56] after sulfur treatment at 400 °C, which resulted in significant decrease in surface area. Detailed study on the deactivation of Pt-supported catalyst was also reported by Dawody et al. [57]. They suggested that three sites (Pt sites, surface storage sites and bulk storage sites) are responsible for the accumulation of the sulfur-containing species after different SO_2 exposure conditions.

However, there are to our knowledge, no studies available in literature that has examined the effect of long term aging with sulfur at low temperature on DME, CO and propane oxidation as well as steam reforming and WGS reaction. In this work, we focus on the effect of aging in inert and sulfur atmosphere of Pt/Al_2O_3 catalyst and the resulting activity on different oxidation/steam reforming reactions (DME, propane, propene and CO). The sulfur aging is conducted at low temperature and for 22 h. The influence of the presence of water in the feed was also investigated in this paper. In addition, the fresh and aged catalysts were characterized with BET, XRD and SEM-EDX.

2. Experimental

2.1. Catalyst synthesis

In this study, Pt/Al_2O_3 wash-coated monolith catalysts were used. The synthesis procedure consists of two main steps: preparation of the Pt-based catalyst in the first step and the washcoating of monoliths with the catalyst powder in the second step. Firstly, γ-Al_2O_3 (Puralox Sasol SBa-200) as catalytic support and $Pt(NO_3)_2$ (W.C. Heraeus GmbH, 15.63 wt.%) were used as starting materials in the synthesis of 1 wt.% Pt/Al_2O_3 catalyst powder by conventional wetness impregnation method. γ-Al_2O_3 powder (pre-calcined at 750 °C for 2.5 h) was slowly added to the noble metal precursor solution under continuous stirring at room temperature and the pH of the obtained solution was kept at 2 by adding diluted solution of HNO_3. The slurry was then freeze-dried in liquid nitrogen for 24 h at 0.9 Pa using ScanVac Cool Safe™ instrument in order to remove the accumulated water. The resulting catalyst powder was ground into agate mortar and calcined at 500 °C for 2 h. In the second step of the preparation procedure, the calcined catalyst powders were deposited on the monoliths. The monoliths (20 mm length, 22 mm diameter) were cut from a honeycomb cordierite structure with a channel density of 400 cpsi and calcined at 500 °C for 2 h prior to the washcoating. A mixture containing a solid phase (95 wt.% Pt/Al_2O_3 catalyst +5 wt.% boehmite Disperal D) and liquid phase (1:1 water:ethanol) was used to washcoat the monolith substrates. The immersing of slurry, drying and heating (550 °C for 1–2 min) procedures were repeated until the desired amount of wash-coat was reached. An amount of 724 mg for fresh (non-aged) sample, 789 mg for Catalyst 1 (used for high temperature aging in Ar) and 776 mg for Catalyst 2 (used for low temperature sulfur aging) were deposited. Finally, 1 wt.% Pt/Al_2O_3 monoliths were calcined at 500 °C for 2 h.

2.2. BET surface area and pore size distribution

The textural properties of crushed, calcined monolith samples were measured by physisorption of N_2 at −196 °C using Micromeritics ASAP 2010 instrument. The samples were first degassed at 225 °C under vacuum conditions for 3 h and about 0.5 g powder of crushed monoliths samples were used for the measurements. Specific BET surface area (S_{BET}) was calculated from the adsorption data in the relative pressure range of 0.05–0.2. The pore size distributions curves were calculated from the analysis of the desorption branch of the isotherm using Barrett–Joyner–Halenda (BJH) algorithm.

2.3. XRD

XRD experiments of the crushed empty, fresh (degreened) and aged samples were performed in a Bruker AXS D8 Advance X-ray powder diffractometer with CuKα radiation (λ = 1.542 Å) at room

temperature. The XRD spectra were registered in the 2θ range of 5 and 90° with an increment step of 0.025°.

2.4. SEM coupled with EDX

In order to characterize the catalyst morphology as well as its surface composition and distribution, an FEI Quanta 200 FEG ESEM microscope equipped with an Oxford Inca Energy Dispersive X-ray (EDX) system was used. Element map SEM/EDX was used to get information regarding the sulfur content in the sulfur aged sample.

2.5. Pt dispersion measurements

The platinum dispersion on Pt/Al_2O_3 was determined by CO chemisorption at 25 °C. Prior to each CO measurement, the catalyst was heated to 450 °C in Argon and a flow of 2% H_2 was introduced in the reactor for 30 min. After fast cooling to room temperature in the same reducing atmosphere, the sample was maintained in inert conditions for 10 min for removal of hydrogen. The CO adsorption experiment was performed at room temperature using two CO pulses. The catalyst was first exposed to 100 ppm CO for 20 min where CO is adsorbed on the catalytic surface. After short time (500 s) flushing in inert atmosphere to remove weakly bonded CO, the second pulse is conducted using same amount of CO for 10 min. During the second pulse, the re-adsorption of CO occurs and weakly bonded CO is adsorbed. The amount of chemisorbed CO was taken as the difference between the total CO uptake (from the first exposure) and the physisorbed CO (during the second pulse). A ratio of 0.8 CO/Pt was used for dispersion calculations [58,59]. Platinum particle sizes were calculated from the dispersion by assuming that the shape of the supported particles is hemispherical [60]. The total flow in these experiments was 1000 mL min^{-1} and the reactor used is described in the next section.

2.6. Catalytic activity measurements

The catalytic activity tests, the aging treatment and the dispersion measurements of the synthesized Pt-based catalysts were performed in a horizontal tubular quartz flow reactor (800 mm length with an inner diameter of 22 mm) at atmospheric pressure. The reactor is surrounded by an insulated heating coil, which is controlled by a Eurotherm temperature controller. The monolith catalyst was placed inside the reactor tube and the quartz wool was wrapped around the catalyst sample, in order to prevent gas passing around the catalyst. Two K-type thermocouples were inserted into the reactor. One thermocouple is located about 10 mm in front of the monolith to control the inlet gas temperature. A second thermocouple is placed in the center of the monolith to measure the sample temperature. The total gas flow during the experiments was 3500 mL min^{-1}, resulting in a space velocity of 30,300 h^{-1} (based on the monolith volume), and was produced by a set of mass flow controllers (Bronkhorst). Argon was used as inert gas. Water was added using a controlled evaporation mixing (CEM) system from Bronkhorst, where the evaporator is heated to 110 °C. All lines were heated and maintained at 200 °C to prevent water condensation. A MultiGas™ 2030 HS FTIR instrument was used to measure the species.

The fresh catalysts were first degreened at 500 °C with a gas mixture of 600 ppm CO, 8% O_2 and 5% H_2O for 2 h. After degreening, the monoliths were subjected to the experiments described in Sections 2.8–2.11. Before each catalytic activity test, the samples were pretreated using the following sequences: (a) heating to 400 °C in Ar for degreened sample and 500 °C for aged catalysts; (b) exposure to 8% O_2 at 400 or 500 °C for 10 min; (c) flushing with Ar at same temperature for 5 min; (d) flowing with 2% H_2 at 400 or 500 °C for 10 min; (e) keeping in Argon at same temperature for 5 min; (f) cooling down in Ar to the target temperature.

2.7. Aging procedure

Two different aging procedures were used, high temperature dry aging treatment in inert atmosphere and low temperature sulfur aging treatment. For the thermal aging, Catalyst 1 was aged at different temperatures (600, 700 and 800 °C) for 2 h in inert atmosphere (Ar). It should be mentioned that in order to emphasize the relevance in the catalytic activity and comparison between fresh and aged catalyst, the obtained results after aging in Ar at 800 °C were only showed in this study, since the results obtained after aging at 600 and 700 °C are similar with the degreened catalyst. Catalyst 2 was aged at 250 °C in a gas mixture consisting of 500 ppm NO, 8% O_2, 5% H_2O, with addition of 30 ppm SO_2 for 22 h. The reaction temperature was first raised to 100 °C in Ar and the sample was exposed to a mixture of 500 ppm NO, 8% O_2 and 5% H_2O for 30 min. After increasing the temperature to 250 °C in same mixture, the sample was maintained in same conditions for 5 min. The sulfur aging was started when 30 ppm SO_2 were added in the gas feed mentioned above. After aging, the catalyst was kept at 250 °C for 20 min in inert atmosphere followed by cooling to room temperature. It should be mentioned that the metal dispersion measurements and the catalytic tests for desired reactions were performed after both aging types. Directly after the aging, CO chemisorption experiments were conducted, where the catalyst is pretreated with 2% H_2 for 30 min at 450 °C.

2.8. DME oxidation in presence/absence of water in the feed

After pretreatment (see Section 2.6), the catalysts were subjected to the DME oxidation experiment. The samples were exposed to 300 ppm DME and 8% O_2 with/without 5% H_2O in the feed at 100 °C for 20 min. The reaction temperature was then increased to 400 °C (for degreened sample) and 500 °C (for aged catalysts) with a rate of 10 °C min^{-1} in a DME + O_2 (with/without H_2O) mixture. At 400 and 500 °C, respectively, the reaction temperature was maintained for 5 min. Thereafter, the catalysts were purged for 5 min in Ar.

2.9. Propane oxidation in the presence/absence of water in the feed

After pretreatment of the catalyst, the propane oxidation experiments were performed according to the following procedure. The samples were exposed to 200 ppm propane and 8% O_2 with/without 5% H_2O at 100 °C for 20 min; the reaction temperature was increased to 400 °C (for degreened sample) and 500 °C (for aged samples) with a rate of 10 °C min^{-1} in same mixture; the catalysts were kept for 5 min in same atmosphere at desired reaction temperature, followed by flowing in inert gas for 5 min.

2.10. CO oxidation in presence/absence of water in the feed

The catalysts were exposed to a gas mixture of 600 ppm CO and 8% O_2 at 100 °C for 20 min. It should be noted that due to the high activity in the presence of 5% H_2O (100% conversion at 100 °C), 2% H_2O in the feed was used instead and the experiments were started already at 50 °C. While exposing the catalyst to the reaction mixture, the temperature was ramped to 400 °C (for degreened sample) or 500 °C (for aged samples) with a rate of 10 °C min^{-1} and the samples were maintained at the target temperature for 5 min in same mixture followed by flushing in Argon for 5 min.

Table 1
Specific BET surface area of empty, degreened and aged 1 wt.% Pt/Al_2O_3 catalyst.

Monolith sample	S_{BET} (m^2/g crushed monolith)	Total pore volume (cm^3/g)
Empty[a]	0.8	0.003
Fresh[b]	61.6	0.192
Catalyst 1[c]	50.1	0.158
Catalyst 2[d]	47	0.156

[a] Calcined commercial cordierite monolith, no catalyst is deposited on it.
[b] Degreened, non-aged sample.
[c] Catalyst 1 was aged at high temperature (800 °C) in Ar for 2 h.
[d] Catalyst 2 was aged in 30 ppm SO_2, 500 ppm NO, 8% O_2 and 5% H_2O at 250 °C for 22 h.

2.11. DME and propane steam reforming (SR). Water-gas shift (WGS) reaction

DME, propane steam reforming reactions and WGS reaction (without oxygen in the feed) were also performed in this study. First the catalyst was pre-treated according to Section 2.6. For DME and propane steam reforming, the catalysts were exposed to 300 ppm DME or 200 ppm propane, respectively, with the addition of 5% H_2O in the feed at 100 °C for 20 min. In case of WGS reaction, 600 ppm CO and 5% H_2O at 100 °C for 20 min were flowed over the catalysts. Thereafter, the reaction temperature was raised to 400 °C (for degreened catalyst) and 500 °C (for aged catalysts) in DME + 5% H_2O or C_3H_8 + 5% H_2O or CO + H_2O, and the samples were kept in the same atmosphere at the desired temperatures for 5 min. Thereafter, the catalysts were flushed with Ar for 5 min.

3. Results and discussion

3.1. Catalyst characterization

The specific BET surface area (S_{BET}) and the pore volume of the empty, degreened and aged 1 wt.% Pt/Al_2O_3 catalysts are summarized in Table 1. Compared with the degreened sample, the surface areas and pore volumes of Ar aged and sulfur aged samples are lower. The aging treatment with Ar and S also had an impact on the pore size distribution (Fig. 1). The non-aged monolith sample has larger volume at a pore diameter of around 10 nm, compared to

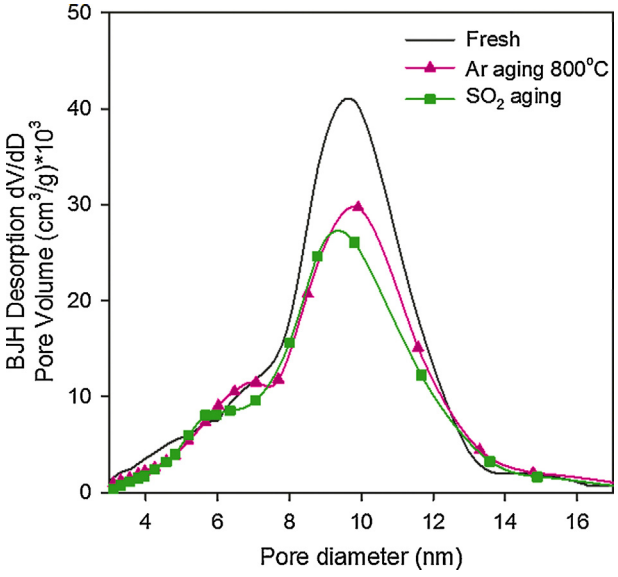

Fig. 1. Pore diameter distribution of fresh (degreened) and aged 1 wt.% Pt/Al_2O_3 monoliths samples. The pore size distributions curves were calculated from the analysis of the desorption branch of the isotherm using BJH algorithm.

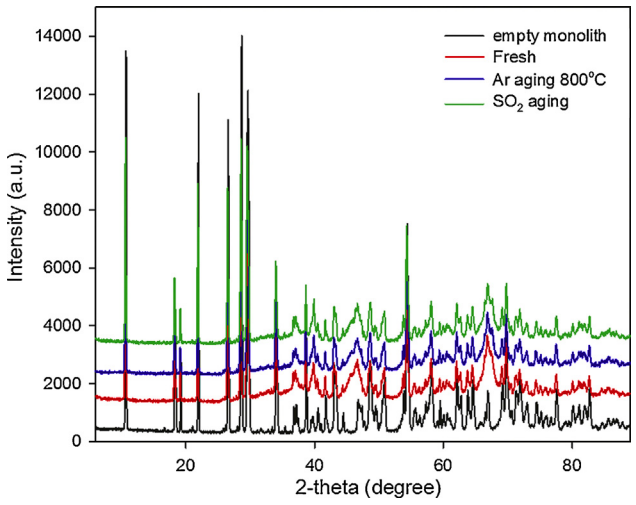

Fig. 2. XRD patterns of the empty, degreened and aged crushed monolith samples. The data were collected at 0.025°/step between $2\theta = 5$ and 90°.

aged samples. The reason for the lower BET area and pore volume for the thermally aged sample is likely that some pores in alumina are collapsed, during thermal aging. For S-poisoned samples, the sulfur likely blocks some pores, which can explain the lowering of the surface area as well as pore volumes.

XRD were also used to characterize the degreened and aged samples. Both amorphous and crystalline phases were identified in the XRD spectra, as is presented in Fig. 2. The most representative crystalline phase with peaks observed in the 2θ range from 9 to 43° are consistent with the standard card file of cordierite (PDF no. 00-013-0294), and is due to that crushed monoliths were used for the analysis. From 2θ between 44° and 84° a mixture of amorphous and crystalline phases are observed revealing different peaks (2θ of 46° is assigned to Pt. The high intensity of the peak at an angle of about 54° corresponds to cordierite substrate. The average crystal sizes of γ-Al_2O_3 were determined based on XRD patterns using Scherrer equation considering the 2θ angle at about 67° [61]. The average crystal size of γ-Al_2O_3 for fresh and aged samples was as following: 7.7 nm for degreened monolith, 7.8 nm for Ar aged sample and 7.9 nm for sulfur aged monolith, respectively. Thus, the crystal sizes are quite similar for all samples.

SEM images of the degreened, Ar aged and sulfur aged catalysts with 200× magnification are presented in Fig. 3 (A–C). From the results in Fig. 3 it is clear that there is a large variation in crystal sizes. Many of the particles seen in SEM are quite large, but it should be noted that particles seen in SEM also could be secondary particles that are agglomerates of primary particles. The fresh catalyst (Fig. 3C) seems to have slightly more small particles, but it could also be only the variations within the samples.

The chemical composition were measured using SEM/EDX, and the results for the degreened, and Ar aged monoliths are shown in Table 2. For sulfur aged monolith sample, the distribution was determined for all three zones, where zone 1, 2 and 3 corresponds to the inlet, middle and end part, respectively. Each zone was also divided into two sub-zones one in the front and one in the end (e.g. sub-zones of 0–1 mm and 5–6 mm for zone 1). The analysis was made by taking an average value of five EDX points, as is seen

Table 2
Elemental composition (wt.%) from SEM/EDX for degreened and Ar-aged monoliths.

Element/sample type	Pt	S	Al	Si	O	C
Degreened	1.1	–	48.3	0.52	46.0	4.1
Catalyst 1	1.6	–	58.3	0.41	34.3	5.1

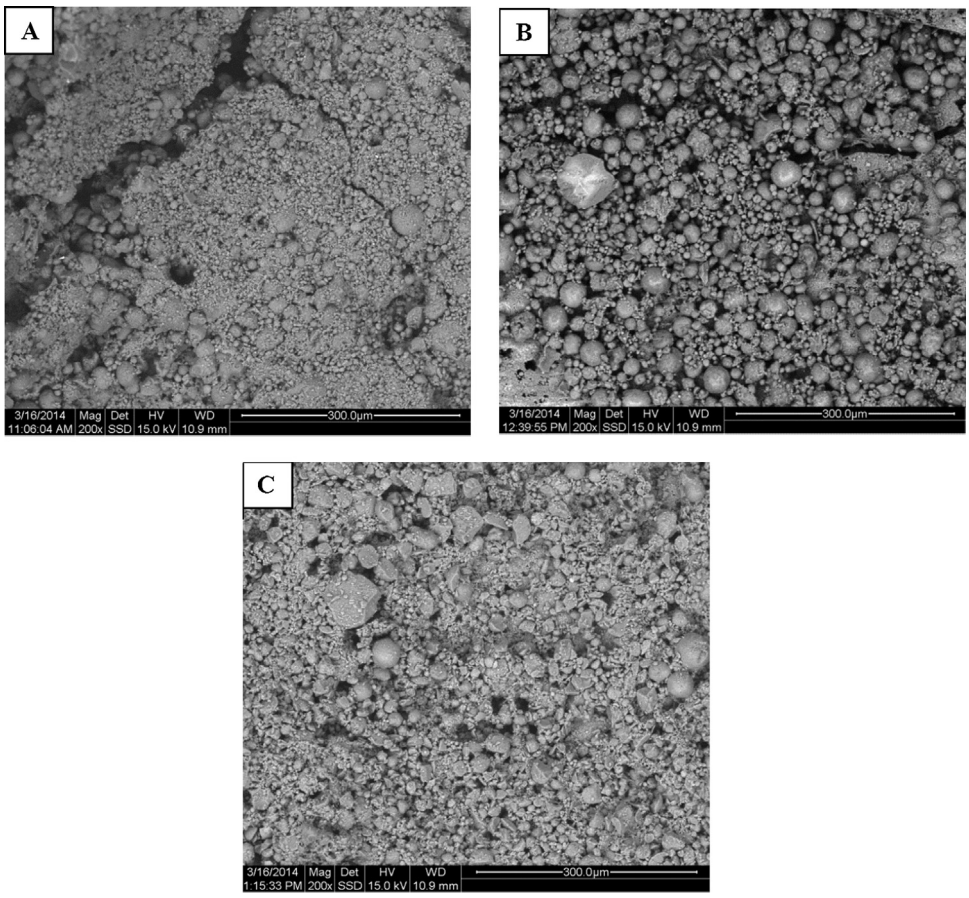

Fig. 3. SEM micrographs magnification 200× at 15 kV of the fresh (A), Ar aged (B) and sulfur aged (C) 1 wt.% Pt/Al_2O_3 monoliths. Working distance (WD) = 10.9 mm with 15 kV for all measurements.

in Fig. 4A. The profile of sulfur amount based on SEM/EDX data along the length of the single channel of the sulfur aged monolith is presented in Fig. 4B. Higher sulfur amount was found in the inlet position of the single channel of the aged sulfur monolith and it decreased with the direction of the flow along the monolith length. The decrease was quite linear and in the end part of the catalyst only small amounts of sulfur were observed. These results clearly show that the sulfur poisoning is not uniform, even though poisoning was conducted during 22 h. Further, it shows that significant amount of sulfur is remaining after hydrogen treatment at 450 °C.

The dispersion of platinum in the prepared catalysts was determined by CO chemisorption at 25 °C according to the procedure described in Section 2.5. The obtained Pt dispersions for fresh and aged samples in inert atmosphere or $SO_2 + NO + O_2 + H_2O$ are depicted in Table 3. The results shows that aging in inert atmosphere gradually decreases the dispersion from 16% for degreened catalyst to 7% after aging at 800 °C in Ar (for Catalyst 1), which corresponds to an average Pt particle size of 6.4 and 14.6 nm, respectively. The data also show that the long term sulfur treatment resulted in a sintering already at 250 °C, giving a dispersion of 7% (for Catalyst 2), the same as after 800 °C aging in Ar. Sintering in this atmosphere at low temperature have been observed previously [55,62,63] and was confirmed with TEM measurements [55].

3.2. Flow reactor tests

The samples were evaluated by means of their catalytic activities in terms of conversions for the reactions described in Section 2.

3.2.1. DME oxidation and DME Steam Reforming (SR)

Fig. 5 shows the effect of the water on the DME oxidation activity of 1 wt.%. Pt/Al_2O_3 degreened catalyst. The addition of 5% H_2O in the feed lowers DME oxidation activity. For example, at 150 °C a conversion of 37% was obtained with only oxygen in the feed, while if water was added the conversion was only 20%. It is likely that water is adsorbed on the platinum and thereby hinders the DME and oxygen adsorption, resulting in lower conversion. It has been found earlier that reactions can be negatively influenced by the presence of water. For example, Marécot et al. [34] observed that water had a negative impact on propane oxidation when using platinum precursors without chlorine and Olsson et al. [64] observed decrease in activity for NO oxidation when water was added.

DME conversion profiles as a function of temperature over fresh (degreened) and aged Pt/Al_2O_3 catalyst are plotted in Fig. 6, where Fig. 6a and b show the effect of aging on DME oxidation in the absence and presence of water, respectively. Quite similar catalytic activities are observed for degreened sample and after aging in Ar at 800 °C, except at higher temperatures where the aging had a negative impact. The catalyst aged in the presence of SO_2 for 22 h has a significantly increased DME conversion, higher than degreened and Argon aged samples both in the presence and the absence of water in the feed. It should be noted that after this aging CO chemisorption is conducted, with a pretreatment in 2% H_2, which removes some of the sulfur [62] and thereafter is the activity measurements conducted. It has previously observed that this long term SO_2 treatment ($NO + O_2 + SO_2$, with or without H_2O, for 22 h at 250 °C), followed by H_2 treatment, has a beneficial effect on NO and propene oxidation over Pt/Al_2O_3 [62,63]. In the present work, we can now show that this beneficial effect is also seen for DME oxidation. Auvray et al.

Table 3
Summary of Pt dispersion and averaged Pt particle size for fresh and aged 1 wt.% Pt/Al_2O_3 catalyst.

Sample	Aging temperature (°C)	Aging time (h)	Aging atmosphere	Pt dispersion[a] (%)	Average Pt particle size[b] (nm)
Catalyst 1	Degreened	–	–	16	6.4
	600	2	Ar	12	8.5
	700	2	Ar	9.5	10.7
	800	2	Ar	7	14.6
Catalyst 2	Degreened	–	–	22	4.6
	250	22	$SO_2 + NO + O_2 + H_2O$	7	14.6

[a] A ratio of 0.8 CO/Pt was assumed [58,59].
[b] Averaged Pt particle size was calculated from the dispersion data by assuming hemispherical particles shapes [60].

[55] suggested that the reason is the formation of larger particles that are more active and they observed a decrease in the Pt dispersion which was confirmed with TEM measurements. Indeed, in this work we also see that the dispersion has dropped significantly from 22 to 7% (see Table 3).

The steam reforming of DME was also examined in order to investigate if that could play a role in the oxidation mechanism. The results are shown in Fig. 5 and it is clear that steam reforming requires much higher temperature than the total oxidation of DME to CO_2. The aging characteristic of this reaction is exhibited in Fig. 6c, and only minor effects of the catalyst aged in Ar at 800 °C (Catalyst 1) and the catalyst aged in sulfur at 250 °C (Catalyst 2) are seen. The experiment after SO_2 aging is repeated and shown in Fig. 6c, giving similar results.

Methanol can be produced as by-product during DME SR. Methanol concentration profile as function of the temperature is depicted in Fig. 7 (it should be noted that for methanol the built-in calibration in the FTIR were used, and there can be some deviation due to that calibration is based on N_2 as carrier gas and we use Ar). Almost no methanol formation is observed for fresh and Ar aged sample. Interestingly, for sulfur aged samples (first and repeated runs), methanol is produced in considerable amount compared to fresh and Ar aged sample, giving two peaks at 300 °C and 397 °C for first run (after SO_2 aging), and 300 °C and 430 °C for 2nd experiment (repeated). For sulfur aged sample, the methanol amount in the product mixture increases with the temperature from 210 to 300 °C, and thereafter decreases from 300 to 350–380 °C for both 1st and 2nd run. Our observation is in agreement with Mathew's study [65], who received highest methanol production for mixed oxides catalysts at 300 °C. In addition, we observe a second methanol peak at higher temperatures, which might be related with the Al_2O_3 sites, since Mathew et al. [65] observe that maximum methanol production occurs at 400 °C for Al_2O_3. However, since methanol is not formed for fresh and Ar aged catalyst, the interaction with sulfur species seems to be crucial. We observe that the selectivity changes in the presence of sulfur and propose that methanol is produced on sulfur sites or sites influenced by stored sulfur. Further, the methanol production is

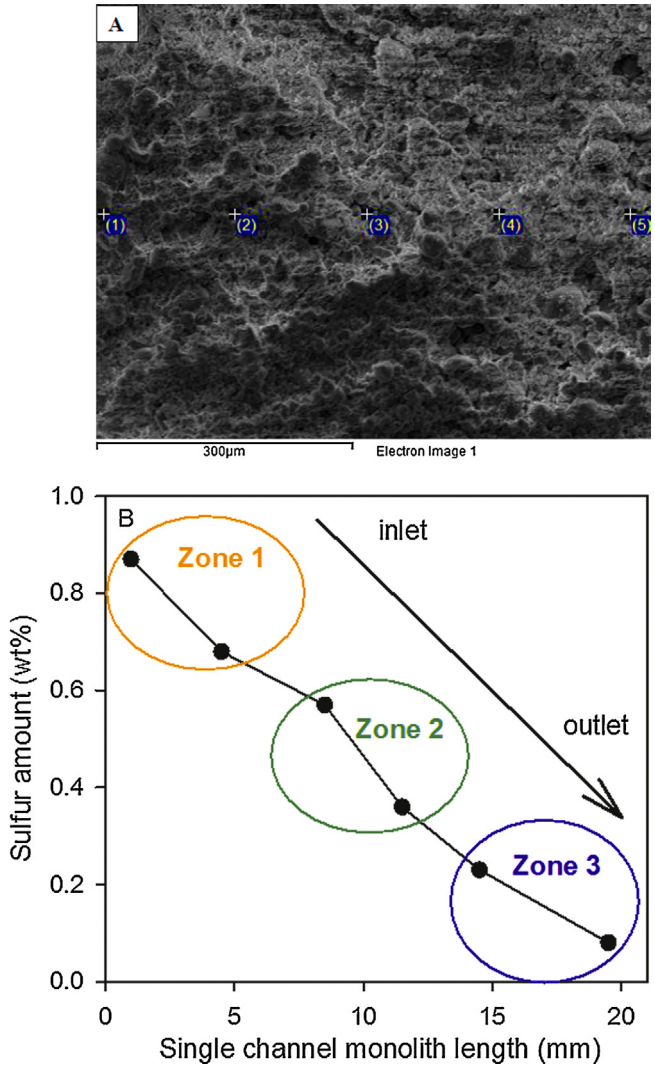

Fig. 4. (A) SEM/EDX analysis of specific zone over sulfur aged monolith sample (e.g. zone 3, channel length of 19–20 mm). (B) Sulfur profile along the length of single channel of monolith (taken from EDX spectra). Three specified locations were chosen for EDX analysis: zone1 (with sub-zones 0–1 mm and 5–6 mm), zone 2 (with 8–9 mm and 11–12 mm) and zone 3 (with 14–15 mm and 19–20 mm), which correspond to the flow direction from inlet to outlet.

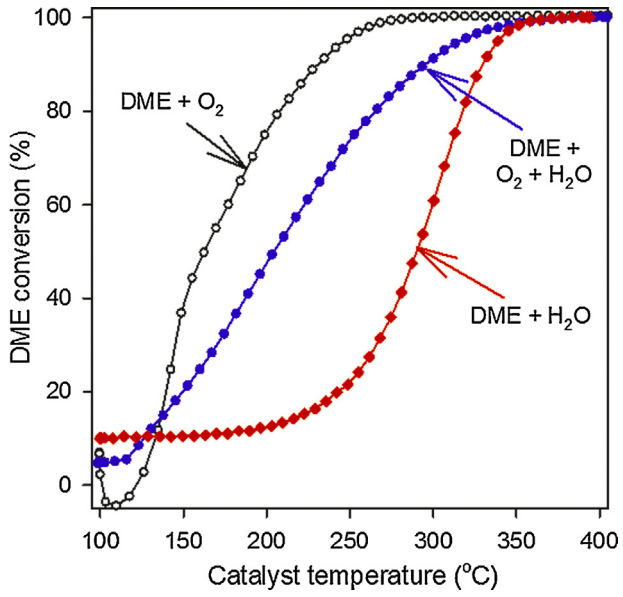

Fig. 5. DME conversion over 1 wt.% Pt/Al_2O_3 fresh monolith for DME oxidation with/without 5% H_2O and DME Steam Reforming (SR). Argon was used as inert balance. Details of the experiments are described in Section 2.

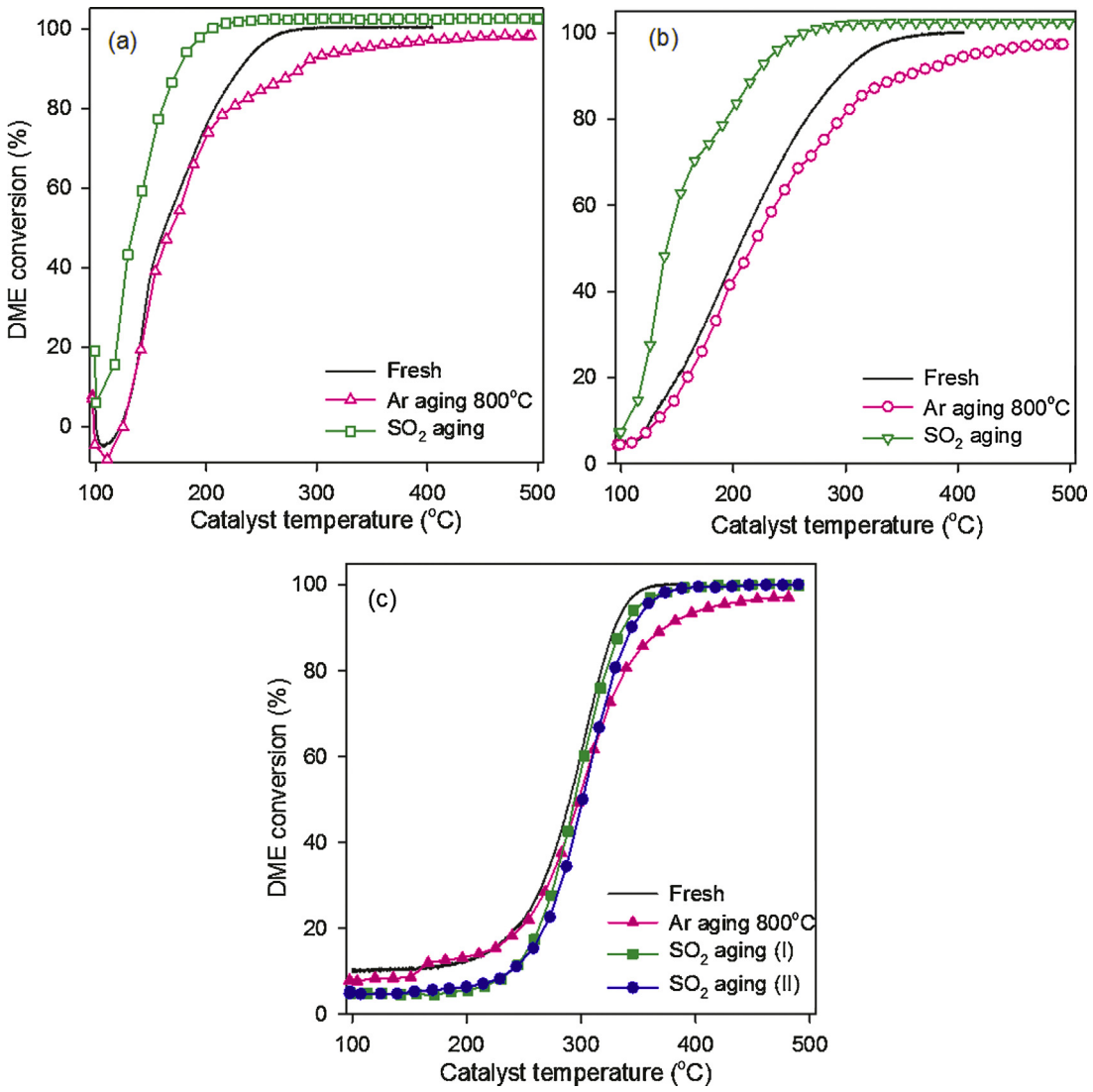

Fig. 6. (a–c) Aging effect on DME conversion over fresh and aged 1 wt.% Pt/Al_2O_3 for DME oxidation (a) without the presence of water, (b) with 5% H_2O and (c) for DME SR. Argon was used as inert balance. Details of the experiments are described in Section 2.

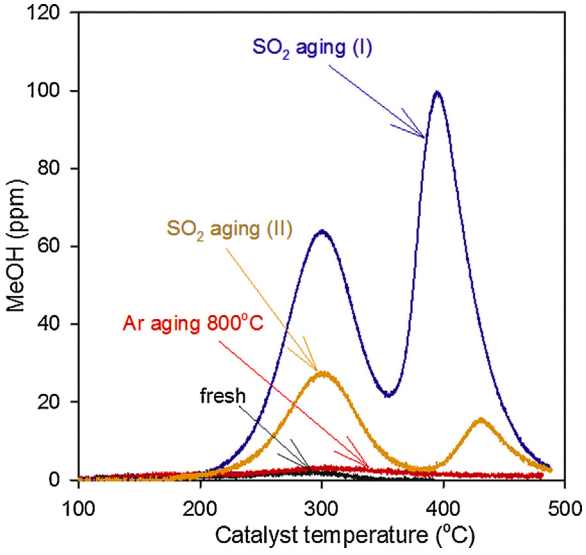

Fig. 7. Methanol concentration profile as function of the catalyst temperature during DME SR. Argon was used as inert balance. Details of the experiments are described in Section 2.

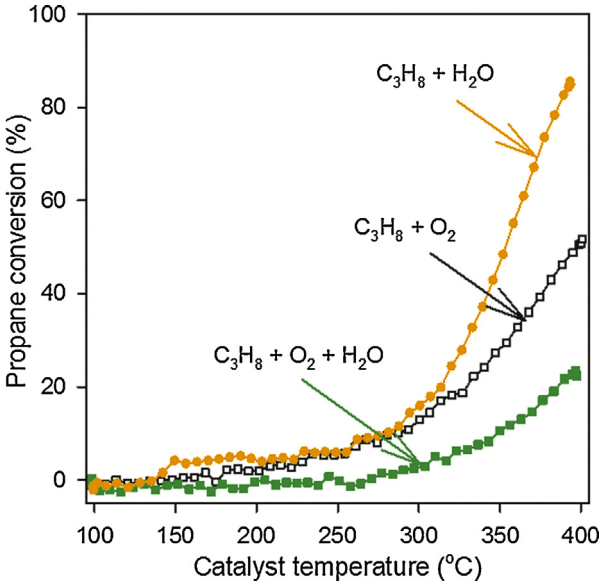

Fig. 8. Propane conversion over 1 wt.% Pt/Al_2O_3 fresh monolith for C_3H_8 oxidation with/without 5% H_2O and propane SR. Details of the experiments are described in Section 2.

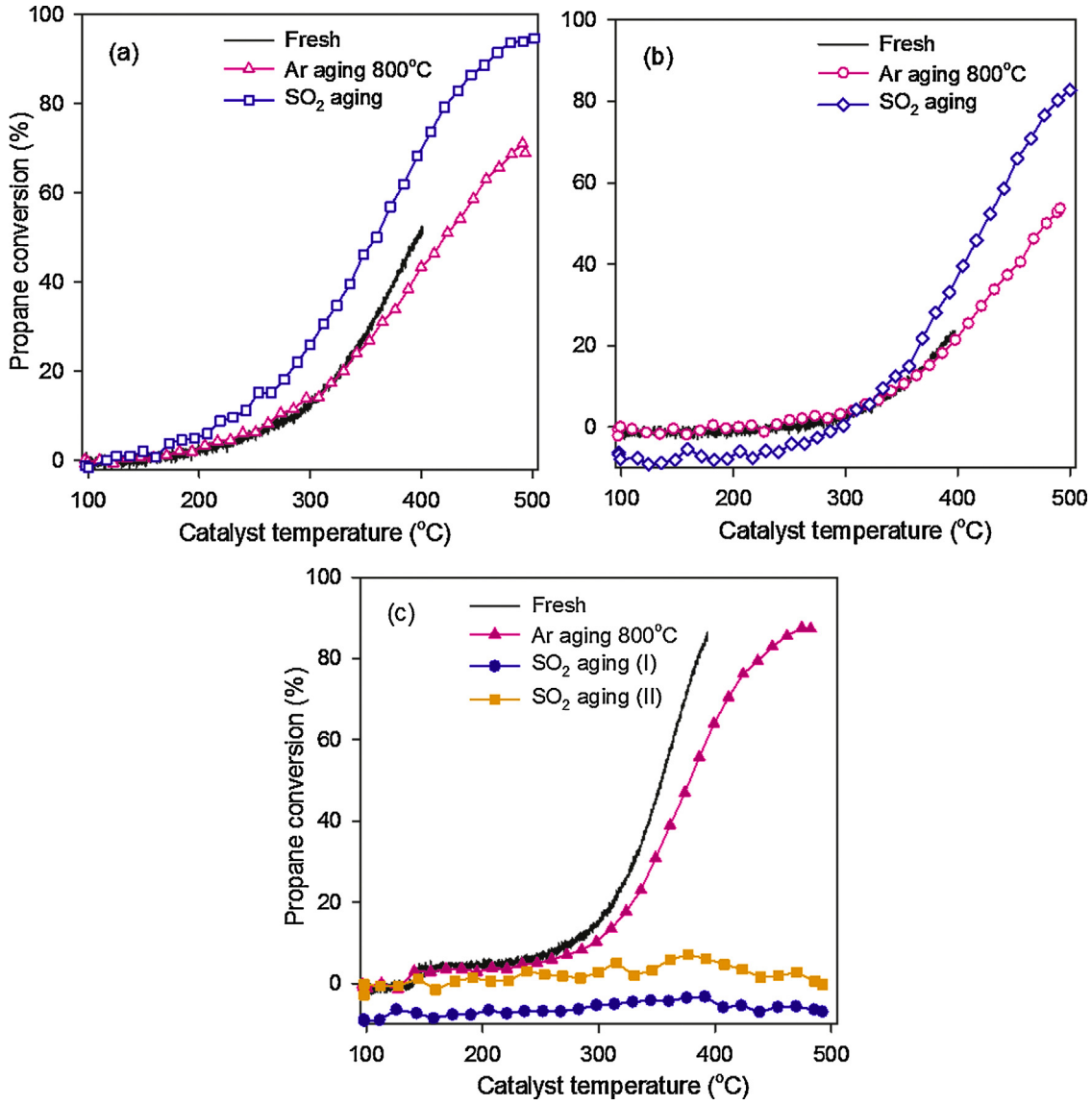

Fig. 9. (a–c) The influence of aging on propane conversion over fresh and aged 1 wt.% Pt/Al_2O_3 catalysts for propane oxidation (a) without the presence of H_2O, (b) with 5% H_2O and (c) for propane SR. Argon was used as inert balance. Details of the experiments are described in Section 2.

decreasing after repeated runs, likely due to that some of the sulfur is removed during the experiment.

3.2.2. *Propane oxidation and propane Steam Reforming (SR)*

Saturated hydrocarbons, such as propane require relatively high temperatures (~400–450 °C) for oxidation and Pt/Al_2O_3 is considered as suitable catalyst for this reaction [20]. Fig. 8 shows the catalytic performances of 1 wt.% Pt/Al_2O_3 catalyst for propane oxidation and steam reforming (SR). A significant negative effect of water is observed during propane oxidation, which is in line with the study by Marécot et al. [34]. Interestingly, the steam reforming reaction occurs at lower temperatures compared to the oxidation reactions. It could be possible that hydrogen is produced from SR and that the hydrogen is combusted during oxygen excess. However, this is not likely the case during oxidative conditions, since the propane oxidation is inhibited by the presence of water. We therefore suggest that the steam reforming is not occurring or with low rate during oxygen excess. Likely the high oxygen coverage on the platinum surface is negative for this reaction.

The effect of catalyst aging on propane activity is demonstrated in Fig. 9. It should be mentioned that the experiments were performed up to the temperature of 400 °C for fresh catalyst and 500 °C for aged samples. At 400 °C, a conversion of 50% was reached over fresh Pt catalyst, while reaching a propane conversion of 42% after aging in Ar at 800 °C was found (Fig. 9a). Thus the aging at 800 °C in Ar only resulted in a small deactivation of the catalyst. However, interesting results are observed after the long-term sulfur aging at 250 °C, as seen for propane oxidation in the absence (Fig. 9a) and presence (Fig. 9b) of water. Note that after aging of the catalyst, there is a pretreatment with H_2 in the chemisorption experiment, which is prior to activity measurements. The sulfur aged catalyst exhibit 71% conversion for propane oxidation in dry conditions at chosen temperature (e.g., 400 °C) (Fig. 9a), while a propane activity of only 40% is observed when water is dosed in the system (Fig. 9b). It means that the aging in SO_2 atmosphere with subsequent reduction has a beneficial effect on the catalytic propane oxidation activity both in presence/absence of water (Fig. 9a and b) and roughly 80–95% propane conversion at 500 °C is obtained in both cases after SO_2 aging. The role of SO_2 on the propane oxidation has been the focus of several studies suggesting that SO_2 promotes propane oxidation due to the formation of the sulfate-based species either at the Pt-alumina interface,

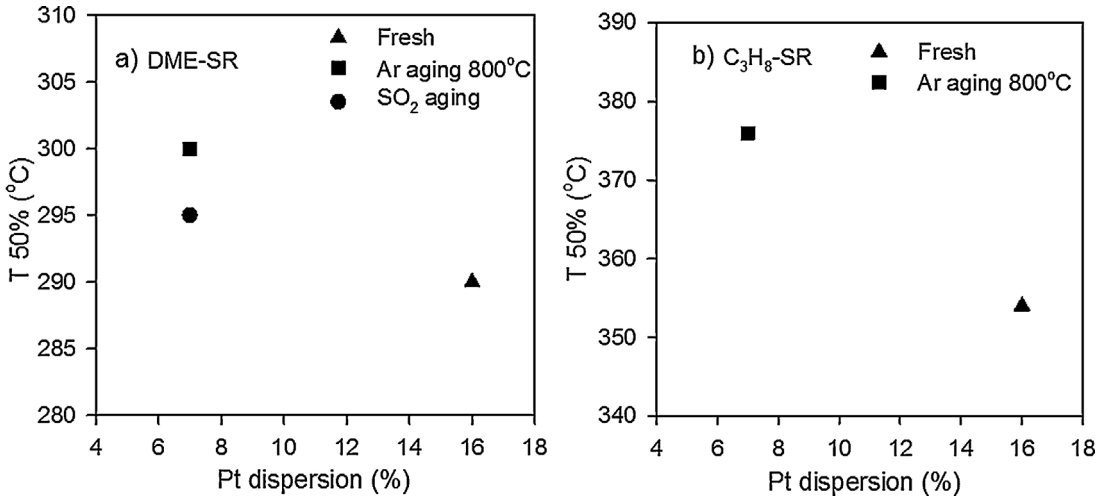

Fig. 10. Pt dispersion as function of temperature for 50% conversion over fresh and aged catalysts on (a) steam reforming of DME and (b) propane steam reforming reaction.

alumina support or platinum sites [33,35,66–68], which facilitates C-H bond activation in propane [67]. Auvray and Olsson [62] observed that there are sulfur species left after hydrogen reduction at 500 °C. Thus, it is likely that some sulfur is left on the surface also in our catalyst after reduction at 450 °C that can have a positive effect for propane oxidation. Indeed, our SEM-EDX results (Fig. 4B) show that significant amount of sulfur is remaining. In addition, it has been observed, that the sulfur aging, followed by reduction, creates larger and more active platinum particles for propene oxidation [62], NO oxidation [55,62] and DME oxidation as shown in this work. It is therefore possible that this is also one of the reasons for the larger activity for propane oxidation. The results for propane steam reforming are shown in Fig. 9c. The catalyst aged at 800 °C in Ar reveals high propane conversion, while almost no propane activity is observed after sulfur aging, as is shown in Fig. 9c. For accuracy, the experiments were repeated twice for SR, giving the same results.

Since Pt particle size play an essential role in the catalytic activity, Fig. 10 shows the dispersion of Pt particles as function of the temperature for the case when 50% conversion is reached on the steam reforming reactions of DME and propane. Significant effect of the Pt dispersion on the activity is revealed for DME-SR (Fig. 10a), with higher activity for the degreened catalyst. The same trend is found for propane-SR (Fig. 10b) for degreened and Ar aged catalyst. However, it should be noted that for sulfur aged sample, the propane conversion is close to zero for whole temperature range (not shown in Fig. 10b). Thus, dispersion is one important effect for the activity, but the chemical interactions with the sulfur plays a major role for some of the reactions.

Methane can be formed during propane SR as an unwanted product and was therefore measured (note that built-in calibration in the FTIR based on N_2 as carrier gas was used for methane, which can give some discrepancy). Fresh and Ar aged samples give a significant methane formation with maximum concentration of around 55 and 23 ppm methane at 388 °C, while no methane is formed after sulfur aging during the whole temperature range (see Fig. 11). Thus, the methane concentration is about two times lower for the Ar aged sample compared to degreened sample even though, the SR conversion is influenced to a smaller extent. The results clearly show that the selectivity for methane production is changed due to the aging.

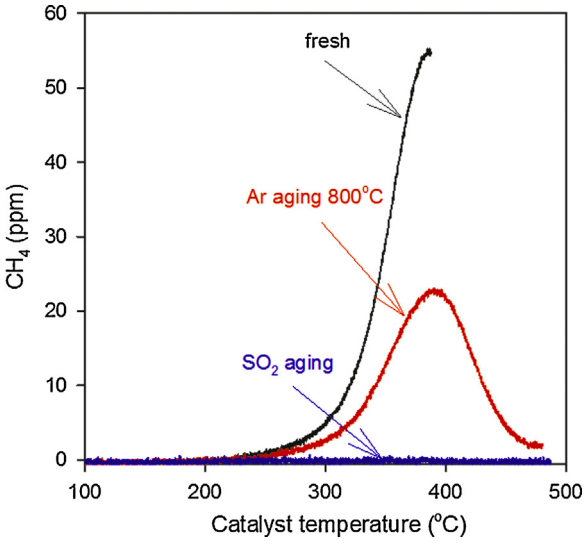

Fig. 11. Methane formation versus temperature during propane SR. Argon was used as inert balance. Details of the experiments are described in Section 2.

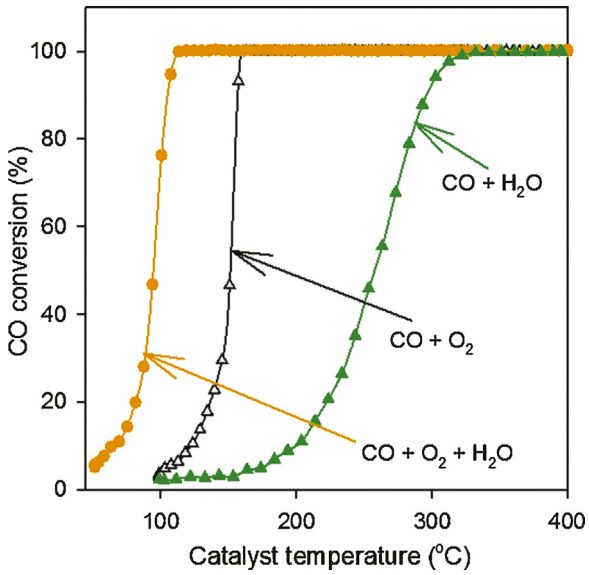

Fig. 12. CO conversion over 1 wt.% Pt/Al_2O_3 fresh monolith for CO oxidation. The temperature of 50 °C and 2% H_2O were employed for CO oxidation, due to 100% conversion at 100 °C with 5% H_2O. Details of the experiments are described in Section 2.

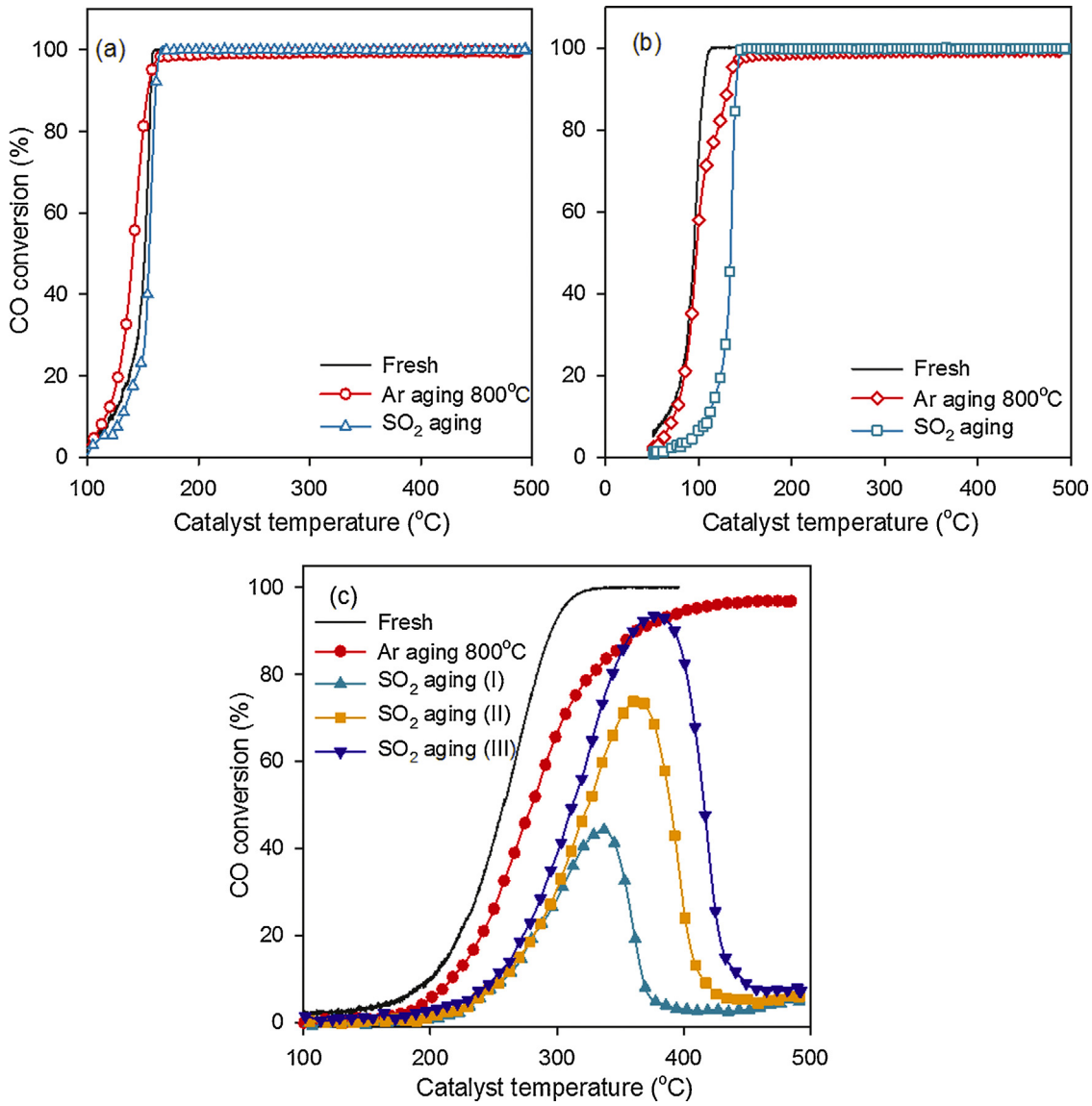

Fig. 13. (a–c) Aging effect on CO conversion over fresh and aged 1 wt.% Pt/Al_2O_3 catalyst for CO oxidation (a) without the presence of H_2O, (b) with 5% H_2O and (c) for CO WGS reaction. Details of the experiments are described in Section 2.

Interestingly, the sulfur aging completely blocks the active sites responsible for steam reforming, while the sites active for oxidation has an increased activity. These results show that these two reactions occur on different sites. For WGS reaction it is suggested that CO is activated on the noble metal, while water is activated by the support [43,69]. We suggest that this is also the case for SR and based on the SEM-EDX results there are still sulfur left on the catalyst after the sulfur aging and regeneration with H_2. We propose that these species inhibit the water activation on alumina and thereby hinders the SR reaction. Another, interesting feature is that steam reforming using DME proceeds with very little deactivation (Fig. 6c), while for propane steam reforming no activity is observed (Fig. 9c) after sulfur aging. One possible explanation could be based on the molecule structure of these compounds; specifically the difference could be that the DME has an ether bond in the molecule, while propane is a saturated stable hydrocarbon, which influences the mechanism for the steam reforming.

3.2.3. *CO oxidation and water gas shift (WGS) reaction*

The catalytic oxidation of CO occurs on platinum surfaces with CO and oxygen adsorbed on the noble metal surface. For WGS reaction it is suggested that CO is activated by the noble metal and that water is activated by the support [43,69]. CO adsorbs on noble metal surfaces more strongly than oxygen [70]. From mechanistic point of view, CO will completely cover Pt catalyst surface at low temperatures due to its strong adsorption behavior and as consequence CO oxidation is inhibited. When increasing temperature (above 100–120 °C) desorption of CO occurs with a decrease in the CO surface coverage, which facilitates oxygen adsorption, resulting in increased oxygen surface coverage and thereby the CO oxidation reaction starts. Fig. 12 shows the light-off curves for the oxidation of CO as a function of temperature for fresh catalyst in the presence and the absence of water in the feed. An increase in CO conversion is observed with an increase in temperature and the conversion is complete below 200 °C. The CO profile is in agreement with other reported studies [71,72]. The addition of 2% H_2O to the feed results in a significant increase in activity. We also examined 5% H_2O (results not shown here), but 100% conversion were obtained already from 100 °C, which is why the water concentration was lowered. The positive effect of water is in line with results presented by Nibbelke et al. [73], who observed both for Pt/Al_2O_3 and a commercial $Pt/Rh/CeO_2/Al_2O_3$ that water enhanced

the CO oxidation. This was also observed by Muraki et al. [74] on Pt/Al_2O_3.

A possible reason for this increase in CO oxidation activity in the presence of water could be WGS reaction to produce H_2 and CO_2 from CO and H_2O and the subsequent combustion of H_2, since hydrogen is very easily oxidized over Pt catalysts. We therefore examined WGS reaction, and the results are depicted in Fig. 12. It is clear that the WGS reaction is less active compared to CO oxidation and therefore the WGS is not the reason for the improved CO oxidation in the presence of water. For propane oxidation (Fig. 8) water had an opposite effect compared to CO, i.e. inhibited the oxidation. One difference between CO and propane is the presence of oxygen in CO. However, it is not enough with only presence of oxygen in the molecule in order to have the promotional effect on the oxidation reactions by water, since DME also contains oxygen but its oxidation was inhibited by water (Fig. 5). Nibbelke et al. [73] suggests that dissociative adsorption of oxygen is the rate determining step in CO oxidation and proposed that the effect of water on $Pt/Rh/CeO_2/Al_2O_3$ was to increase the rate for this dissociative adsorption on ceria. This was suggested to occur through the production of OH-groups from water on ceria, and these OH-groups reacted with O_2 molecularly adsorbed in order to produce oxygen-atoms. However, in our catalyst ceria is not present and this path is therefore not possible. Muraki et al. [74] suggested that the beneficial effect of water on CO oxidation over Pt/Al_2O_3 is that water may decrease the CO poisoning of the platinum surface, which is one possibility for our catalysts.

Similar activities are observed for fresh and aged samples for CO oxidation, when water is not present in the feed (Fig. 13a). However, when water is introduced to the feed (Fig. 13b), a small deactivation of the catalyst is observed at high conversions for the case where the catalyst was thermally aged in Ar at 800 °C. Moreover, SO_2 aging, followed by hydrogen regeneration, influences CO conversion negatively when water is present in the feed (Fig. 13b). The oxidation activity for CO sharply increases and reaches almost complete CO conversion (~100%) at 120 °C for fresh sample and at 150 °C for aged samples when water is present in the feed (Fig. 13b).

WGS reaction over Pt/Al_2O_3 catalyst was also studied in this work. Fig. 13c shows the results for the WGS reaction over fresh and aged samples. For the thermally aged sample, the CO conversion versus temperature is lower compared to the fresh sample. Thus, the WGS reaction is more sensitive toward thermal aging compared to CO oxidation. Interestingly, completely different behavior of the CO conversion profile for the WGS reaction is noticed for Pt-based catalyst aged in $SO_2 + NO + O_2 + H_2O$ (22 h at 250 °C) and subsequently reduced in H_2 at 450 °C. The conversion of CO starts at a higher temperature and reaches a maximum of 44% at 337 °C and thereafter the conversion decreases and reaches 2% conversion at 408 °C. For accuracy, we reported the results of three repeated experiments after the aging in SO_2. All experiments show similar trend, but the activity is increasing for each WGS experiment. One possible explanation for this is gradual removal of sulfur from the alumina sites during reaction conditions. The long-term sulfur treatment has two effects on the catalyst: (i) causes platinum migration and sintering (see Table 3), which is also observed in other studies [54,55] and (ii) some sulfur species are remaining on the surface, as seen by SEM-EDX. As described above it is proposed that in the WGS reaction, water is activated by the support and CO on the noble metal [43,69]. We therefore propose that there are residues of sulfur remaining on alumina, which inhibit the water activation on alumina needed for the WGS. Interestingly, the conversion decreases at higher temperature. Deactivation by sulfur was also occurring for steam reforming of propane, but propane was even more sensitive to the sulfur blocking. Surprisingly, the steam reforming of DME was not affected, indicating that the SR with ether follows another reaction mechanism.

4. Conclusions

The effect of the presence/absence of water in the feed for Pt-based catalyst was examined in this study. In addition, the aging behavior for Pt/Al_2O_3 was investigated. The aging was performed at 600, 700 and 800 °C in Argon for 2 h and at 250 °C in $SO_2 + NO + O_2 + H_2O$ for 22 h. After each aging step, Pt dispersion measurements and various oxidation reactions (DME, propane and CO), as well as DME- and propane-SR and WGS reactions were investigated.

The fresh and aged catalysts were characterized with BET, SEM with EDX and XRD. Both the Ar and sulfur aging treatments resulted in decreased BET surface area and pore volume compared to degreened catalyst. For the thermally aged sample the high temperature probably results in collapsing of some pores, since XRD gave similar average crystal size. For the sulfur aged catalyst the decreased area and volume is likely due to blocking of some pores with sulfur. Further, SEM/EDX analysis showed higher sulfur amount in the inlet position of the single channel of the sulfur aged monolith and it decreased linearly with the direction of the flow along the monolith length.

For the catalyst aged in Ar the dispersion decreased gradually, and after aging in sulfur the Pt dispersion decreased dramatically compared to fresh catalyst, which means that SO_2 exposure leads to platinum migration, which has also been observed in earlier studies.

The CO conversion is higher compared to the conversion of DME and C_3H_8, and the oxidation activity follows the trend: CO > DME > C_3H_8. The addition of water to the gas mixture results in a decreased conversion for DME and propane oxidation, while an increase for CO oxidation. It is interesting to note, that both CO and DME contains oxygen, but the beneficial effect is isolated to CO. One hypothesis for the increase in activity for CO oxidation in the presence of water is the occurrence of WGS and that the produced H_2 is easily combusted. However, our results show that WGS reaction occurs at a significantly higher temperature, which is why this hypothesis is not likely. It is possible that water reduces the CO inhibition of platinum and thereby increases the conversion, as suggested in the literature. Also DME and propane SR over Pt/A_2O_3 catalyst were examined in this work. For the catalyst aged in Ar, 50% conversion was obtained for WGS reaction, DME- and propane-SR at 280, 300 and 380 °C, respectively. Thus, WGS is the most active reaction.

Thermal aging of the Pt/Al_2O_3 catalyst in Ar for 2 h at 800 °C, resulted in only quite small deactivation for the examined reactions. The largest deactivation was found for the WGS reaction, but also for this reaction the deactivation was low. The dispersion after the thermal aging was 7%, which was the same as after the long-term sulfur aging, but interestingly the behavior is completely different. After the sulfur aging and subsequent hydrogen regeneration, the DME and C_3H_8 oxidation is strongly promoted, especially propane oxidation in the presence of water, while CO oxidations is slightly inhibited in the presence of water. Previous studies [54,55,62] have shown the beneficial effect of this treatment at low temperature with sulfur, followed by hydrogen regeneration, for both NO oxidation and propene oxidation. Since the dispersion is the same after thermal aging (7%) and sulfur aging, we propose that the sulfur aging results in formation of platinum particles that are more active for oxidation of NO, propane, propene and DME. In addition, for propane oxidation the actual sulfur species may also play a role for the increased activity.

The effect of the sulfur aging, and subsequent hydrogen reduction, on the WGS and steam reforming was studied. It only had a minor effect on DME-SR, while complete deactivation for propane steam reforming was observed after the sulfur aging. However, after sulfur aging substantial amount of methanol was formed during DME-SR, which were not observed for degreened or Ar aged sample. For WGS reaction with CO, the sulfur aging (and following H_2 reduction), resulted in a decreased activity at lower temperature, followed by a maximum conversion of 44% at 337 °C, and thereafter decreased conversion, e.g. only 2% conversion were remained at 408 °C. This experiment was repeated three times, showing the same trend but an increase in activity after each repetition. SEM/EDX showed that substantial amounts of sulfur were remaining on the catalyst. In addition, it has been proposed earlier that water is activated by the support and CO on the noble metal in the WGS reaction [43,69]. We therefore propose that the residues of sulfur remaining on alumina inhibit the water activation on alumina needed for the WGS. During repeated experiments some sulfur might be removed in reaction conditions, which causes the increase in WGS activity when repeating the experiment. Interestingly, the WGS after aging exhibits a maximum in conversion, which indicates that there are two paths for WGS: one at low temperature and one at high temperature. Further, we suggest that it is the same reason for the inhibition of the steam reforming of propane after sulfur aging, and subsequent H_2 treatment, i.e. sulfur remaining on alumina hinders the water activation needed for SR. The sulfur aging is more severe for the propane SR compared to the WGS reaction. Interestingly, steam reforming of DME is not affected by the sulfur aging, suggesting that there is another mechanism for steam reforming of DME, where water activation on alumina is not critical.

Acknowledgements

The work is financially supported by Swedish Foundation for Strategic Research (F06-0006) and Swedish Energy Agency (32077-1) and was performed at the Competence Center for Catalysis, which is hosted by Chalmers University of Technology and financially supported by the Swedish Energy Agency and the member companies AB Volvo, ECAPS AB, Haldor Topsøe A/S, Scania CV AB, Volvo Car Corporation AB and Wärtsilä Finland Oy.

References

[1] T. Tzamkiozis, L. Ntziachristos, Z. Samaras, Atmos. Environ. 44 (2010) 909–916.
[2] T.A. Semelsberger, R.L. Borup, H.L. Greene, J. Power Sources 156 (2006) 497–511.
[3] W.S. Epling, L.E. Campbell, A. Yezerets, N.W. Currier, J.E. Parks, Catal. Rev. Sci. Eng. 46 (2004) 163–245.
[4] M. Koebel, M. Elsener, M. Kleemann, Catal. Today 59 (2000) 335–345.
[5] M. Koebel, M. Elsener, O. Kröcher, C. Schär, R. Röthlisberger, F. Jaussi, M. Mangold, Top. Catal. 30–31 (2004) 43–48.
[6] S.C. Sorenson, J. Eng. Gas Turbines Power 123 (2001) 652–658.
[7] T. Shudo, H. Yamada, Int. J. Hydrogen Energy 32 (2007) 3066–3070.
[8] C. Arcoumanis, C. Bae, R. Crookes, E. Kinoshita, Fuel 87 (2008) 1014–1020.
[9] V.V. Galvita, G.L. Semin, V.D. Belyaev, T.M. Yurieva, V.A. Sobyanin, Appl. Catal. A 216 (2001) 85–90.
[10] K. Takeishi, H. Suzuki, Appl. Catal. A 260 (2004) 111–117.
[11] T. Kawabata, H. Matsuoka, T. Shishido, D. Li, Y. Tian, T. Sano, K. Takehira, Appl. Catal. A 308 (2006) 82–90.
[12] S. Wang, T. Ishihara, Y. Takita, Appl. Catal. A 228 (2002) 167–176.
[13] Q. Zhang, X. Li, K. Fujimoto, K. Asami, Appl. Catal. A 288 (2005) 169–174.
[14] Q. Zhang, X. Li, K. Fujimoto, K. Asami, Catal. Lett. 102 (2005) 197–200.
[15] Q. Zhang, F. Du, X. He, Z.-T. Liu, Z.-W. Liu, Y. Zhou, Catal. Today 146 (2009) 50–56.
[16] F. Solymosi, J. Cserényi, L. Ovári, Catal. Lett. 44 (1997) 89–93.
[17] B. Solsona, T. García, G.J. Hutchings, S.H. Taylor, M. Makkee, Appl. Catal. A 365 (2009) 222–230.
[18] L. Zhang, D. Weng, B. Wang, X. Wu, Catal. Commun. 11 (2010) 1229–1230.
[19] B. Solsona, I. Vázquez, T. Garcia, T. Davies, S. Taylor, Catal. Lett. 116 (2007) 116–121.
[20] A.C. Gluhoi, N. Bogdanchikova, B.E. Nieuwenhuys, Catal. Today 113 (2006) 178–181.
[21] B. Wang, X. Wu, R. Ran, Z. Si, D. Weng, J. Mol. Catal. A: Chem. 361–362 (2012) 98–103.
[22] V. Balcaen, H. Poelman, D. Poelman, G.B. Marin, J. Catal. 283 (2011) 75–88.
[23] G. Silversmit, H. Poelman, V. Balcaen, P.M. Heynderickx, M. Olea, S. Nikitenko, W. Bras, P.F. Smet, D. Poelman, R. De Gryse, M.-F. Reniers, G.B. Marin, J. Phys. Chem. Solids 70 (2009) 1274–1280.
[24] W.B. Li, J.X. Wang, H. Gong, Catal. Today 148 (2009) 81–87.
[25] J.-Y. Luo, M. Meng, J.-S. Yao, X.-G. Li, Y.-Q. Zha, X. Wang, T.-Y. Zhang, Appl. Catal. B 87 (2009) 92–103.
[26] R. Burch, M.J. Hayes, J. Mol. Catal. A: Chem. 100 (1995) 13–33.
[27] K. Otto, J.M. Andino, C.L. Parks, J. Catal. 131 (1991) 243–251.
[28] X. Wu, L. Zhang, D. Weng, S. Liu, Z. Si, J. Fan, J. Hazard. Mater. 225–226 (2012) 146–154.
[29] T.F. Garetto, E. Rincón, C.R. Apesteguía, Appl. Catal. B 73 (2007) 65–72.
[30] D. Ghita, D.S. Ezeanu, D. Cursaru, P. Rosca, Rev. Chim. 63 (2012) 1296–1300.
[31] Y. Yazawa, H. Yoshida, T. Hattori, Appl. Catal. A 237 (2002) 139–148.
[32] H. Yoshida, Y. Yazawa, T. Hattori, Catal. Today 87 (2003) 19–28.
[33] A.F. Lee, K. Wilson, R.M. Lambert, C.P. Hubbard, R.G. Hurley, R.W. McCabe, H.S. Gandhi, J. Catal. 184 (1999) 491–498.
[34] P. Marécot, A. Fakche, B. Kellali, G. Mabilon, P. Prigent, J. Barbier, Appl. Catal. B 3 (1994) 283–294.
[35] H.C. Yao, H.K. Stepien, H.S. Gandhi, J. Catal. 67 (1981) 231–236.
[36] K. Irani, W.S. Epling, R. Blint, Appl. Catal. B 92 (2009) 422–428.
[37] A. Abedi, R. Hayes, M. Votsmeier, W. Epling, Catal. Lett. 142 (2012) 930–935.
[38] V.G. Milt, S. Ivanova, O. Sanz, M.I. Domínguez, A. Corrales, J.A. Odriozola, M.A. Centeno, Appl. Surf. Sci. 270 (2013) 169–177.
[39] S. Salomons, M. Votsmeier, R.E. Hayes, A. Drochner, H. Vogel, J. Gieshof, Catal. Today 117 (2006) 491–497.
[40] Y. Liu, M.P. Harold, D. Luss, Appl. Catal. A 397 (2011) 35–45.
[41] C.W. Corti, R.J. Holliday, D.T. Thompson, Appl. Catal. A 291 (2005) 253–261.
[42] C. Ratnasamy, J.P. Wagner, Catal. Rev. Sci. Eng. 51 (2009) 325–440.
[43] A.D. Allian, K. Takanabe, K.L. Fujdala, X. Hao, T.J. Truex, J. Cai, C. Buda, M. Neurock, E. Iglesia, J. Am. Chem. Soc. 133 (2011) 4498–4500.
[44] P. Panagiotopoulou, D.I. Kondarides, Catal. Today 112 (2006) 49–52.
[45] G.G. Olympiou, C.M. Kalamaras, C.D. Zeinalipour-Yazdi, A.M. Efstathiou, Catal. Today 127 (2007) 304–318.
[46] A.K. Neyestanaki, F. Klingstedt, T. Salmi, D.Y. Murzin, Fuel 83 (2004) 395–408.
[47] A.K. Datye, Q. Xu, K.C. Kharas, J.M. McCarty, Catal. Today 111 (2006) 59–67.
[48] P. Loof, B. Stenbom, H. Norden, B. Kasemo, J. Catal. 144 (1993) 60–76.
[49] J. Yang, V. Tschamber, D. Habermacher, F. Garin, P. Gilot, Appl. Catal. B 83 (2008) 229–239.
[50] P.C. Flynn, S.E. Wanke, J. Catal. 37 (1975) 432–448.
[51] P.C. Flynn, S.E. Wanke, J. Catal. 34 (1974) 390–399.
[52] J. Kim, C. Kim, S.-J. Choung, Catal. Today 185 (2012) 296–301.
[53] S.K. Matam, E.V. Kondratenko, M.H. Aguirre, P. Hug, D. Rentsch, A. Winkler, A. Weidenkaff, D. Ferri, Appl. Catal. B 129 (2013) 214–224.
[54] L. Olsson, H. Karlsson, Catal. Today 147 (2009) S290–S300.
[55] X. Auvray, T. Pingel, E. Olsson, L. Olsson, Appl. Catal. B 129 (2013) 517–527.
[56] T. Kolli, T. Kanerva, M. Huuhtanen, M. Vippola, K. Kallinen, T. Kinnunen, T. Lepistö, J. Lahtinen, R.L. Keiski, Catal. Today 154 (2010) 303–307.
[57] J. Dawody, M. Skoglundh, L. Olsson, E. Fridell, J. Catal. 234 (2005) 206–218.
[58] B. Engler, E. Koberstein, D. Lindner, E. Lox, Stud. Surf. Sci. Catal. 71 (1991) 641–655.
[59] C.C. Chang, J. Catal. 53 (1978) 374–385.
[60] A. Boubnov, S. Dahl, E. Johnson, A.P. Molina, S.B. Simonsen, F.M. Cano, S. Helveg, L.J. Lemus-Yegres, J.-D. Grunwaldt, Appl. Catal. B 126 (2012) 315–325.
[61] S. Kureti, W. Weisweiler, J. Non-Cryst. Solids 303 (2002) 253–261.
[62] X.P. Auvray, L. Olsson, Ind. Eng. Chem. Res. 52 (2013) 14556–14560.
[63] X. Auvray, L. Olsson, Catal. Lett. (2013) 1–10.
[64] L. Olsson, M. Abul-Milh, H. Karlsson, E. Jobson, P. Thormählen, A. Hinz, Top. Catal. 30–31 (2004) 85–90.
[65] T. Mathew, Y. Yamada, A. Ueda, H. Shioyama, T. Kobayashi, Appl. Catal. A 286 (2005) 11–22.
[66] G. Corro, R. Montiel, C.L. Vázquez, Catal. Commun. 3 (2002) 533–539.
[67] K. Ruth, M. Hayes, R. Burch, S. Tsubota, M. Haruta, Appl. Catal. B 24 (2000) L133–L140.
[68] K. Wilson, C. Hardacre, R.M. Lambert, J. Phys. Chem. 99 (1995) 13755–13760.
[69] V.M. Shinde, G. Madras, Int. J. Hydrogen Energy 37 (2012) 18798–18800.
[70] S.H. Oh, G.B. Fisher, J.E. Carpenter, D.W. Goodman, J. Catal. 100 (1986) 360–376.
[71] D.J. Suh, C. Kwak, J.-H. Kim, S.M. Kwon, T.-J. Park, J. Power Sources 142 (2005) 70–74.
[72] D.H. Kim, M.S. Lim, Appl. Catal. A 224 (2002) 27–38.
[73] R.H. Nibbelke, M.A.J. Campman, J.H.B.J. Hoebink, G.B. Marin, J. Catal. 171 (1997) 358–373.
[74] H. Muraki, S.-I. Matunaga, H. Shinjoh, M.S. Wainwright, D.L. Trimm, J. Chem. Technol. Biotechnol. 52 (1991) 415–424.